BULLETIN
OF THE
KOREAN CHEMICAL SOCIETY

VOLUME 19, NUMBER 9
SEPTEMBER 20, 1998

BKCS 19(9) 895-1018
ISSN 0253-2964

Feature Article

Synthesis, Characterization, and Crystal Structures of Iron(II) and Manganese(II) Complexes with 4,7-bis(2-pyridylmethyl)-1-thia-4,7-diazacyclononane

Delong Zhang, Daryle H. Busch*, and Nathaniel W. Alcock†

Department of Chemistry, University of Kansas, Lawrence, Kansas 66045, USA
†Department of Chemistry, University of Warwick, Coventry CV4 7AL, United Kingdom
(Received July 9, 1998)

A new synthesis has been developed for 1-thia-4,7-diazacyclononane and the complexation behavior of a particular derivative has been explored. The pentadentate ligand 4,7-bis(2-pyridylmethyl)-1-thia-4,7-diazacyclononane ([9]N_2Spy_2) and its iron(II) and manganese(II) complexes were prepared and characterized. Magnetic moments of 5.17 and 5.90 μ_B, respectively, indicate that the iron(II) and manganese(II) complexes are high spin. Charge transfer transitions (d-π^*) occur for $[Fe(II)([9]N_2Spy_2)(X)]^{n+}$ at 27027, 25000, and 24390 cm^{-1} for X=H_2O, Cl^-, and OH^-, respectively. In acetonitrile solution, the cyclic voltammogram of the manganese(II) complex exhibits a redox couple at 0.92 V *vs.* NHE while the redox potentials for $[Fe(II)([9]N_2Spy_2)(X)]^{n+}$ are 0.70, 0.66, and 0.37 V *vs.* NHE for X=H_2O, Cl^-, and OH^-, respectively. The d-π^* charge transfer energy and Fe(II)/Fe(III) redox potential for $[Fe(II)([9]N_2Spy_2)(X)]^{n+}$ increase in the same order: $H_2O > Cl^- > OH^-$. The crystal structures of the iron(II) and manganese(II) complexes reveal that the metal ions are six-coordinate, binding to four nitrogen atoms and a sulfur atom from the pentadentate ligand, as well as a chloride anion, with the chloride and sulfur atoms in *cis* positions. The two metals have similar coordination geometries, which are closer to trigonal prismatic than octahedral. In both iron and manganese complexes, the M-N(sp^3) *trans* to Cl^- is 0.07 Å longer than the one *cis* to Cl^-, and M-N(sp^2) *trans* to S is 0.05 longer than the one *cis* to S atom.

Introduction

In many metalloenzymes and metalloproteins, the coordination spheres around the metal centers are not saturated, and substrates interact with the metals through the vacant coordination position during enzymatic reactions. For example, it has been suggested that the open coordination sites in iron superoxide dismutase (Fe-SOD) are essential for the reactivity of superoxide dismutase.[1-4] Therefore, to use metal complexes to mimic the active sites in metalloenzyme, pentadentate or tetradentate ligands are desirable because such metal as iron and manganese usually have coordination numbers of six. During our search for effective superoxide dismutase mimics,[5] we synthesized 1,4-bis(2-pyridylmethyl)-1,4,7-diazacyclononane ([9]N_3py_2), a pentadentate ligand (see Structure), but found that the Fe(II) complex is not stable to oxygen in aqueous solution, and that the oxidized product is inactive toward superoxide.[5c] If the NH group on the triazacyclononane ring is replaced by a sulfur, the iron(II) complex should be less easily oxidized since sulfur usually stabilizes the +2 oxidation state of iron. These considerations defined 4,7-bis(2-pyridylmethyl)-1-thia-4,7-diazacyclononane ([9]N_2Spy_2) as our target ligand (Structure).

The preparations of [9]N_2Spy_2 and its Cu(II), Ni(II), Pt(II), and Pd(II) complexes, and the crystal structures of the metal complexes have previously been reported.[6,7] The Cu(II), Pt(II), and Pd(II) complexes approximate square pyramidal geometries with the sulfur at the apical position while the Ni(II) complex includes an additional H_2O, giving a slightly

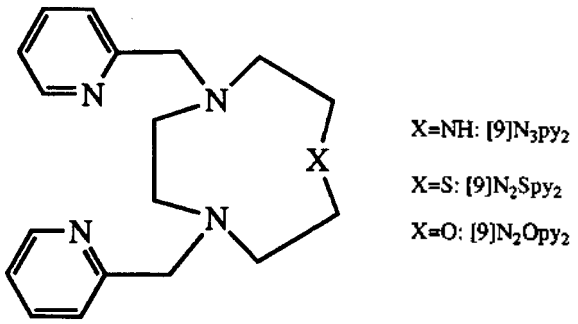

Structure 1

distorted octahedral geometry. We report here a new method for the preparation of 1-thia-4,7-diazacyclononane ([9]aneN$_2$S) and the synthesis of the Fe(II) and Mn(II) complexes of the pentadentate derivative, 4,7-Bis(2-pyridylmethyl)-1-thia-4,7-diazacyclononane ([9]N$_2$Spy$_2$). The magnetic properties, electronic spectra, electrochemistry, and crystal structures of the new complexes are also be discussed.

Experimental Section

Chemicals

Ethylene glycol (98%), *p*-tosyl chloride (98%), and 2-picolyl chloride hydrochloride (98%) were purchased from Aldrich chemical company. Sodium sulfide nonahydrate and 2-hydoxylethylamine were obtained from Baker Chemical Company and Fisher Scientific Company, respectively. All organic solvents were of reagent grade and were used without further purification. Deionized water with conductance of 1.79×10^{7} ohm·cm was used to prepare aqueous solutions.

Synthesis

2-Tosylaminoethyl-*p*-toluenesulfonate (2). The literature procedure[8,9] was modified and used for preparation of the compound. HOCH$_2$CH$_2$NH$_2$ (61 g, 1 mol) in 300 mL of pyridine was added dropwise to *p*-toluenesulfonyl chloride (400 g, 2.1 mol) in 1.2 L of pyridine at −30 °C under stirring. The mixture was further stirred for 5 hours at −30 °C and 6 hr at 0 °C before being slowly poured into 5 L of ice-water with vigorous stirring. The yellow precipitate was collected by suction filtration and stirred in another 5 L of cold water for 30 min before it was filtered, washed with water, and dissolved in chloroform (1 L). After the organic phase was separated and dried over anhydrous sodium sulfate, chloroform was removed on a rotary evaporator, and the product was further dried in a vacuum oven at 50 °C. Yield: 330 g, 90%. ^{1}H NMR: 2.37 (singlet, 3H), 2.40 (singlet, 3H), 3.17 (quartet, 2H), 4.01 (triplet, 2H), 5.23 (triplet, 1H), 7.23 (doublet, 2H), 7.29 (doublet, 2H), 7.66 (doublet, 2H), and 7.70 ppm (doublet, 2H). The NMR spectrum of the product was used as the criterion for purity and further purification was unnecessary.

***p*-Tosylaziridine (3).** According to the reported procedure,[8,9] compound **2** (106 g, 0.28 mol) was suspended in toluene and 32 g (0.6 mol) of KOH (300 mL H$_2$O) was added dropwise with vigorous stirring. After the addition of potassium hydroxide, the mixture was stirred for 3 hours. The organic phase was separated and dried over anhydrous sodium sulfate. The toluene solution was evaporated on a rotary evaporator and the residue was dried in a vacuum oven. The NMR spectrum indicated that the product was fairly pure. ^{1}H NMR: 2.36 (singlet, 4H), 2.44 (singlet, 3H), 7.35 (doublet, 2H), and 7.83 ppm (doublet, 2H). ^{13}C NMR: 22.0, 27.8, 128.3, 130.1, 135.2, and 145.1 ppm.

***N,N'*-Ditosyl-3-thia-1,5-diaminopentane N,N'-Disodium Salt (4).** The crude product (**3**) was added to 700 mL of absolute ethanol, dissolving upon heating. To the solution, sodium sulfide nonahydrate (36.7 g, 0.153 mol) was added and the solution was refluxed overnight. After it was cooled to room temperature, the solution was filtered, and the filtrate evaporated to obtain a pale yellow solid. In order to confirm that compound **4** was obtained, water was added to a small amount of the solid, and the pH of the solution was adjusted to about 7 with HCl to convert the disodium salt to free ditosylamine. The mixture was extracted with $CDCl_3$, and the $CDCl_3$ solution was separated and dried over anhydrous sodium carbonane. The NMR spectrum identified the compound in the $CDCl_3$ solution as *N,N'*-ditosyl-3-thia-1,5-diaminopentane (**5**). ^{1}H NMR (in $CDCl_3$): 2.28 (singlet, 6H), 2.42 (triplet, 4H), 2.93 (quartet, 4H), 5.51 (singlet, 2H), 7.16 (doublet, 4H), 7.62 ppm (doublet, 4H). Crude **4** was practically pure and was used for the following ring closure reaction without further purification.

***N,N'*-Ditosyl-1-thia-4,7-diazacyclononane (6).** Compound **4** was dissolved in 1.2 L of DMF, forming a dark red solution. Under stirring, 53 g (0.143 mol) of 1,2-bis(tosyl(oxy))ethane in 300 mL of DMF was slowly added over a period of 12 hours at 70 °C. The pale red brown solution was further stirred for 30 hrs before the volume of the solution was reduced to 500 mL by rotary evaporation. Under vigorous stirring, the resulting solution was slowly added to ice-water to yield a pale yellow precipitate. The solid was collected by suction filtration, washed with water and dissolved in 800 mL of chloroform. The $CHCl_3$ solution was dried over anhydrous sodium sulfate for 3 hrs, followed by evaporation, producing a mixture of a solid and a thick sticky oil, which was dried in a vacuum oven to obtain a solid. The crude product was dissolved in 700 mL of hot acetonitrile and the solution was evaporated to 150 mL on a rotary evaporator to obtain a nearly white solid, which was collected and washed with 50 mL of acetonitrile. Yield: 15.5 g. The filtrate was further reduced in volume (to 80 mL) and put in a refrigerator for one day, yielding another 3.9 g of product. Total yield: 19.4 g (43 mmol), 31% based on **2**. This satisfactory yield can be improved by recovering additional product from the filtrate. ^{1}H NMR (in $CDCl_3$): 2.44 (singlet, 6H), 3.13 (triplet, 4H), 3.37 (singlet, 4H), 3.50 (triplet, 4H), 7.33 (doublet, 4H), and 7.67 ppm (doublet, 4H). ^{13}C NMR (in $CDCl_3$): 21.6, 30.2, 52.1, 53.8, 127.3, 129.9, 134.6, and 143.8 ppm. Anal. Calc. for $C_{20}H_{26}N_2O_4S_3$: N, 6.16; C, 52.84; H, 5.76. Found: N, 6.30; C, 53.00; H, 5.80.

1-Thia-4,7-diazacyclononane di(hydrobromide) (7). To 15 g (33 mmol) of compound **6**, acetic acid (150 mL) and hydrobromic acid (49%, 150 mL) were added, and the mixture was refluxed for three days. The volume of the resulting dark brown solution was reduced to one sixth, and

300 mL of a mixture of diethyl ether and ethanol (v/v: 7 : 1) was added to precipitate the detosylated product. Yield: 9.5 g or 94%. ^{1}H NMR (D_2O): 3.11 (triplet, 4H), 3.50 (triplet, 4H), 3.73 (singlet, 4H). ^{13}C NMR (in D_2O): 27.7, 42.5, and 44.5 ppm. Anal. Calc. for $C_6H_{16}N_2SBr_2 \cdot 0.5H_2O$: N, 8.83; C, 22.73; H, 5.40. Found: N, 8.81; C, 22.70; H, 5.49.

4-7-Bis(2-pyridylmethyl)-1-thia-4,7-diazacyclononane (8). Compound 7 (0.68 g, 2.1 mmol) and 0.72 g (4.4 mmol) of picolyl chloride hydrochloride were dissolved in 15 mL of water. After the solution was cooled to 0 °C, 10 mL of sodium hydroxide solution (16 mmol) was added, with stirring, to raise the pH to 13. Stirring was continued overnight with some oil forming after three hours. Chloroform (30 mL) was added to extract the product (in another experiment, the aqueous solution was decanted before chloroform was added to dissolve the oily residue). After separating and drying (Na_2CO_3), removal of the chloroform resulted in a brown yellow oil. Yield: 0.58 g, 82%. The NMR spectrum indicated that the product was pure. ^{1}H NMR (in $CDCl_3$): 2.67 (singlet, 4H), 2.96 (triplet, 4H), 3.12 (triplet, 4H), 3.85 (singlet, 4H), 7.16 (triplet, 2H), 7.52 (doublet, 2H), 7.67 (triplet, 2H), and 8.51 (doublet, 2H). ^{13}C NMR (in $CDCl_3$): 32.0, 56.1, 59.0, 64.3, 121.9, 123.3, 136.4, 148.8, and 159.9 ppm.

[Fe([9]N_2Spy$_2$)Cl]CF_3SO_3 (9). In a glove box, $FeCl_2$ (0.22 g, 1.74 mmol) in 2 mL of methanol was added to a methanol solution (5 mL) of **8** (0.58 g, 1.74 mmol) under stirring. The mixture was stirred under reflux for 1 hour. After cooling to 40 °C, the solution was clarified by filtration. With stirring, a clear methanol solution of sodium trifluoromethanesulfate (0.60 g, 3.5 mmol) was added to the filtrate. Golden crystals were obtained when the resulting solution was slowly cooled to room temperature. The mass spectrum exhibited a strong peak at m/e=419, corresponding to [Fe([9]N_2Spy$_2$)Cl]$^+$. Anal. Calc. for $C_{19}H_{24}ClF_3O_3N_2S_2Fe$: N, 9.85, C, 40.12; H, 4.25. Found: N, 9.68; C, 39.82; H, 4.10.

[Mn([9]N_2Spy$_2$)Cl]CF_3SO_3 (10). The ligand (**8**) (0.32 g, 10 mmol) was dissolved in 2 mL of methanol, and $MnCl_2H_2O$ (0.20 g, 1.0 mmol) in 2 mL of methanol was slowly added with stirring. The mixture was boiled for 1 hr and stirred for another 2 hrs. After cooling the solution to room temperature and filtering, a clear methanol solution of sodium trifluoromethanesulfate (2.0 mmol) was added, with stirring, producing an off-white precipitate. This was collected by suction filtration, washed with methanol, and dried in air. Elemental analysis suggested that the product contained a small amount of sodium chloride, so this crude product was dissolved in 15 mL of acetonitrile to form a cloudy solution. It was difficult to remove the particles by filtration since they were very fine, but after the cloudy solution was left undisturbed for a day, the particles settled to the bottom of the vial. The clear solution was decanted and evaporated in air to obtain X-ray quality crystals. Yield: 0.41 g (0.71 mmol), 71%. The mass spectrum exhibited a strong peak at m/e=418, corresponding to [Mn([9]N_2Spy$_2$)Cl]$^+$. Anal. Calc. for $C_{19}H_{24}ClF_3O_3N_2S_2Mn$: N, 9.87; C, 40.18; H, 4.26. Found: N, 9.68; C, 40.32; H, 4.65.

Instrumentation

Magnetic susceptibilities were determined by Evans' method[10,11] on a QE 300 Plus NMR instrument. Several milligrams of [M([9]N_2Spy$_2$)Cl](CF_3SO_3) were dissolved in 0.500 mL of deuterated DMSO in an NMR tube before an inner tube with a narrow end containing pure deuterated acetonitrile was inserted into the solution containing the complex. Diamagnetic corrections were made using Pascal's constants.[12] ^{1}H and ^{13}C NMR spectra were determined with a QE 300 Plus spectrometer.

Electronic spectra of the metal complexes in acetonitrile solutions were recorded on a Hewlett Packard 84552 diode array spectrophotometer (HP) with an 89500 UV/Vis Hewlett Packard ChemStation; scan ranges: 190-820 nm. Acetonitrile and aqueous solutions were used, and the aqueous solution was prepared under nitrogen. Under a nitrogen atmosphere, Fe[9]N_2Spy$_2$(OH) was prepared by adding two equivalents of sodium hydroxide to an aqueous solution of the iron(II) complex. Conductances of the complexes (about 1 mM in acetonitrile) were measured with a YSI Model 35 conductance meter.

Electrochemical experiments were performed on a Princeton Applied Research Model 175 programmer and Model 173 potentiostat. The output was recorded on paper using a Houston Instruments recorder. A glassy carbon electrode, a silver wire, and a platinum wire were used as working, reference, and secondary electrodes, respectively. Acetonitrile and aqueous solutions (1-2 mM) were used in the experiments, and all the experiments were performed under nitrogen. Supporting electrolytes: 0.1 M tetrabutylammonium tetrafluoroborate (0.1 M) for acetonitrile solution and 0.1 M $NaClO_4$ for aqueous solutions. The potentials vs. NHE were determined by using ferrocene as internal reference in acetonitrile solution.

Table 1. Crystal data for complexes (**9**) and (**10**)

Compound	[Fe([9]N_2Spy$_2$)Cl](CF_3SO_3) **9**	[Mn([9]N_2Spy$_2$)Cl](CF_3SO_3) **10**
Formula	$C_{19}H_{24}N_4F_3O_3S_2ClFe$	$C_{19}H_{24}N_4F_3O_3S_2ClMn$
Molecular wt	568.8	563.9
Crystal system	Orthorhombic	Orthorhombic
Space group	$P2_12_12_1$	$P2_12_12_1$
a	8.105(6) Å	8.152(2) Å
b	13.370(7) Å	13.438(3) Å
c	20.848(13) Å	20.750(4) Å
V	2259 Å^3	2273 Å^3
Z	4	4
D_{cal} (g cm^{-3})	1.67	1.65
l	0.71069 Å	0.71073 Å
μ(MoKα) (mm^{-1})	1.03	0.94
T	250 K	120 K
hkl ranges:	0/9; 0/15; 0/24	−9/7; −13/15; −23/21
Refls: total	2314	9482
Unique	2314	3605
Obs ($I \geq 2\sigma(I)$)	1778	3362
Crystal size	0.059×0.30×0.32	not ecorded
Parameters	298	298
wR2	0.050 (F(obs))	0.079 (F^2, all refls)
R (final)	0.044	0.034
R (all refls)	0.063	0.036
Fourier maxima	0.30	+0.61; −0.35

Table 2. Atom coordinates ($\times 10^4$) and isotropic thermal parameters ($Å^2 \times 10^3$)

(a) for (**9**)

Atom	x	y	z	U
Fe(1)	8520.5(12)	8624.0(7)	7164.9(5)	22(1)*
Cl(1)	6074.9(23)	7727.7(15)	7033.2(10)	40(1)*
S(2)	286.3(28)	4826.1(16)	5521.4(10)	40(1)*
O(21)	15832(8)	4385(6)	6115(3)	59(2)*
O(22)	15163(11)	5542(5)	5266(4)	82(3)*
O(23)	18004(8)	5049(6)	5490(4)	73(3)*
C(O2)	16066(11)	3810(6)	4965(4)	41(3)*
F(21)	14560(8)	3433(5)	4974(3)	81(3)*
F(22)	17102(9)	3073(4)	5098(3)	86(3)*
F(23)	16375(9)	4086(5)	4373(2)	77(2)*
S(1)	8978(24)	7606(13)	8167(9)	30(1)*
C(2)	7733(10)	8468(6)	8634(3)	34(3)*
C(3)	8129(10)	9559(6)	8550(3)	29(3)*
N(4)	8164(7)	9859(4)	7868(3)	24(2)*
C(5)	9566(9)	10561(6)	7733(3)	30(2)*
C(6)	11201(9)	10035(5)	7785(4)	31(2)*
N(7)	11172(8)	9085(4)	7421(3)	24(2)*
C(8)	12022(9)	8271(5)	7771(3)	29(2)*
C(9)	11090(9)	7960(6)	8375(3)	33(2)*
C(10)	6601(9)	10318(6)	7674(3)	30(2)*
C(11)	6499(9)	10437(5)	6956(3)	26(2)*
N(12)	7476(8)	9848(5)	6601(3)	27(2)*
C(13)	7406(11)	9899(6)	5968(4)	37(3)*
C(14)	6304(12)	10529(7)	5654(5)	49(3)*
C(15)	5303(11)	11145(6)	6017(4)	43(3)*
C(16)	5414(10)	11100(6)	6681(4)	36(3)*
C(17)	11949(10)	9210(6)	6788(3)	32(3)*
C(18)	11514(10)	8350(5)	6354(3)	27(2)*
N(19)	9949(8)	8028(5)	6393(3)	30(2)*
C(20)	9472(10)	7311(6)	5995(3)	32(2)*
C(21)	10504(11)	6876(7)	5546(4)	38(3)*
C(22)	12101(11)	7191(7)	5531(4)	44(3)*
C(23)	12637(10)	7958(7)	5925(4)	39(3)*

Equivalent isotropic U defined as one third of the trace of the orthogonalised U_{ij} tensor.

(b) for (**10**)

	x	y	z	U(eq)
Mn(1)	1458.1(6)	6350.2(4)	2134.2(2)	14(1)
Cl(1)	3914.3(10)	7314.2(7)	2005.1(4)	24(1)
S(1)	994.5(10)	7338.7(7)	3207.8(4)	18(1)
C(2)	2242(4)	6444(3)	3653(2)	19(1)
C(3)	1812(4)	5353(3)	3552(2)	17(1)
N(4)	1781(3)	5067(2)	2859.0(13)	15(1)
C(5)	385(4)	4393(3)	2708(2)	17(1)
C(6)	−1268(4)	4930(3)	2769(2)	19(1)
N(7)	−1269(4)	5885(2)	2416.6(13)	16(1)
C(8)	−2064(4)	6695(3)	2793(2)	18(1)
C(9)	−1124(4)	6988(3)	3397(2)	19(1)
C(10)	−2070(4)	5787(3)	1782(2)	19(1)
C(11)	−1644(4)	6632(3)	1331(2)	16(1)
N(12)	−48(3)	6936(2)	1343.9(13)	17(1)
C(13)	425(4)	7651(3)	943(2)	19(1)
C(14)	−634(4)	8112(3)	514(2)	21(1)
C(15)	−2261(4)	7815(3)	509(2)	24(1)
C(16)	−2762(4)	7061(3)	921(2)	20(1)
C(17)	3362(4)	4587(3)	2673(2)	19(1)
C(18)	3521(4)	4484(3)	1953(2)	18(1)
N(19)	2618(3)	5091(2)	1585.2(14)	18(1)
C(20)	2763(4)	5049(3)	941(2)	22(1)
C(21)	3844(4)	4397(3)	641(2)	25(1)
C(22)	4772(4)	3769(3)	1020(2)	24(1)
C(23)	4615(4)	3804(3)	1675(2)	21(1)
S(2)	1293.3(11)	9870.3(7)	5510.3(4)	21(1)
O(1)	3025(3)	10078(2)	5476.9(14)	34(1)
O(2)	765(3)	9459(2)	6115.5(12)	29(1)
O(3)	226(3)	10602(2)	5236(2)	41(1)
C(24)	1063(4)	8822(3)	4955(2)	24(1)
F(1)	1383(3)	9093(2)	4352.2(10)	38(1)
F(2)	2075(3)	8075(2)	5102.0(12)	40(1)
F(3)	−460(3)	8457(2)	4966.1(12)	41(1)

Crystal Structure Determination

Crystal data for the complexes of iron(II) and manganese (II) are given in Table 1. The two complexes are isomorphous, though the atomic coordinates relate to different origins. Data were collected with a Siemens R3m four circle diffractometer in ω-2θ mode (**9**) or an Enraf-Nonius CAD-4 with the FAST area detector of the SERC Crystallographic service (**10**). Temperatures were maintained with an Oxford Cryosystems Cryostream Cooler.[13] Maximum 2θ was 50°. For (**9**) backgrounds were measured at each end of the scan for 0.25 of the scan time. Three standard reflections were monitored every 200 reflections, and showed no decrease during data collection. Unit cell dimensions and standard deviations were obtained by least-squares fit to 27 reflections ($15° < 2T < 18°$). Reflections were processed using profile analysis to give 2314 unique reflections, of which 1778 were considered observed ($I/\sigma(I) \geq 2.0$). These were corrected for Lorentz, polarization and absorption effects (by the analytical method using ABSPSI;[14] minimum and maximum transmission factors were 0.78 and 0.94. For (**10**), any decay was corrected in data processing and no absorption correction was made.

For both, systematic reflection conditions h00, h=2n; 0k0, k=2n; 00l, l=2n: indicated space group $P2_12_12_1$. The structures were solved by direct methods (TREF) using SHELXTL PLUS. Anisotropic displacement parameters were used for all non-H atoms. Hydrogen atoms were given fixed isotropic displacement parameters, U=0.08 $Å^2$ (**9**); 1.2* attached atom (**10**), and were inserted at calculated positions and not refined. The absolute structures of the individual crystals chosen was checked by refinement of a δf'' multiplier (value 1.03(8)) (**9**) or by refinement of an absolute structure parameter (value −0.03(2)) (**10**). For **9**, final refinement was on F by least squares methods with a weighing scheme of the form $W=1/(s^2(F)+gF^2)$ with g= 0.00096. For **10**, refinement was on F^2, using all reflections. The weighing scheme was $w=1/[s^2(Fo^2)+(0.033P)^2]$ where $P=(Fo^2+2Fc^2)/3$. The fractional coordinates for the non-hydrogen atoms are listed in Table 2. For **9**, computing was with SHELXTL PLUS[15] on a DEC Microvax-II, and for **10** with SHELXL[16] on a IBM 486 PC. Scattering factors in the analytical form and anomalous dispersion factors were taken from International Tables (stored in the program).

Results and Discussion

Synthesis. The synthesis of 1-thia-4,7-diazacyclononane has been reported in the literature.[7,14,17] In most procedures, the precursor compound, 3-thia-1,5-diaminopentane was either synthesized from aziridine and hydrogen sulfide or purchased (though it is not commonly available). Aziridine is a highly toxic compound and a heart disease suspect.[19] Its high vapor pressure (160 mmHg at 20 °C) makes it especially dangerous. Moreover, hydrogen sulfide gas also is highly toxic, and inconvenient to use. Recently, Wasielewski *et al.*[7] also reported the preparation of the precursor compound by the reaction of 2-chloroethylamine with sodium sulfide.

In our new method for the preparation of 4,7-bis(2-pyridylmethyl)-1-thia-diazacyclononane (Scheme 1) relatively innocuous reagents are used. Compound **2** was prepared from $HOCH_2CH_2NH_2$ (**1**) following procedures described in literature.[8,9] **2** is practically pure and was not further purified. Compound **3** was prepared almost quantitatively from 2-tosylaminoethyl-*p*-toluenesulfonate. After the removal of the solvent, **3** was combined with half an equivalent of sodium sulfide to form *N,N'*-disodium salt of *N,N'*-Ditosyl-3-thia-1,5-diaminopentane (**4**). Compared with the reaction between sodium sulfide and $ClCH_2CH_2NH_2$, this reaction does not have complicated side reactions, such as polymerization, since the amine groups in the product are protected from further reactions. The reaction gave an essentially pure product, as indicated by the ^1H and ^{13}C NMR spectra of the protonated product (**5**). The reaction between the disodium salt (**4**) and 1,2-bis(tosyl(oxy))ethane to form *N,N'*-ditosyl-1-thia-4,7-diazacyclononane (**6**), not only avoids using the highly toxic reagents, hydrogen sulfide gas and aziridine, but also constitutes a simpler procedure. The preparation of **6** from **2** is basically a one-pot synthesis, except for the removal of solvents at each step. 4,7-Ditosyl-1-thia-4,7-diazacyclononane was purified by recrystallization from acetonitrile. A significant loss of product occurred since it is soluble in acetonitrile. Nevertheless, the cumulative yield of about 30% (for the three-step process) is highly satisfactory, in view of the usual low yield of ring closure reactions.

The detosylation of compound **6** using a mixture of concentrated hydrobromic acid and acetic acid has often been troublesome, sometimes with yields of a few percent, or even zero.[20] In sharp contrast, in this laboratory, the same procedure gave a very impressive 92% yield. The problems encountered in earlier studies may result from loss of product due to its solubility in the supernate (the mixture of hydrobromide acid, acetic acid, ethanol, and diethyl ether). As the procedure for the detosylation of tritosyl-triazamacrocyclic compounds is adapted for use with the analogous ditosyl-thiadiazamacrocyclic compound the differences in the properties of the detosylated products should be considered. This difference in charge (triple for a triazamacrocycle and double for the N_4S analog) may have a dramatic impact on the solubility of the product, with a less polar solvent increasing the yield of the latter. In our procedure, the reaction mixture was evaporated to one-sixth the volume of the original solution to reduce the acid concentration, thereby decreasing the polarity of the mixed

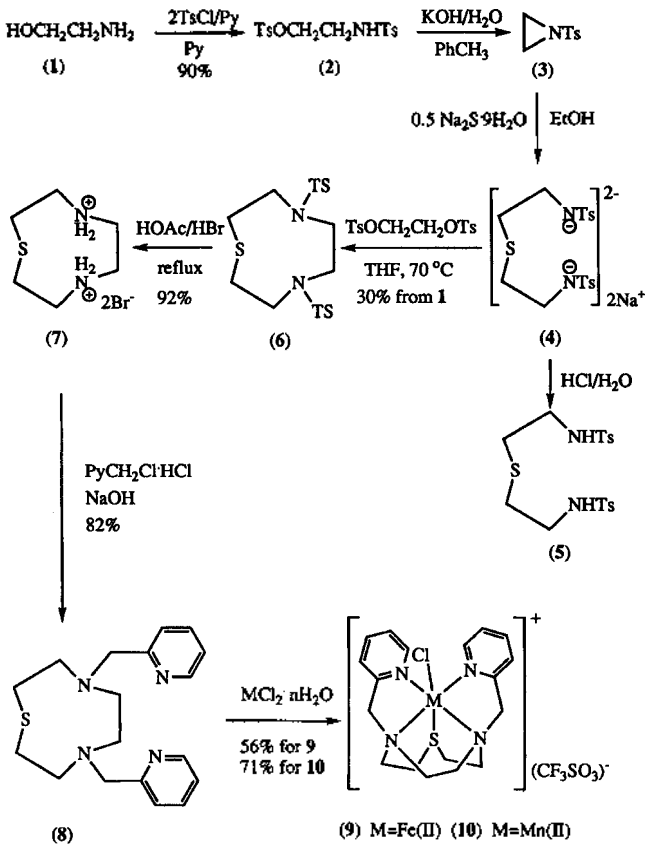

Scheme 1

solvent system. In addition, a larger proportion of diethyl ether was used in the diethyl ether/ethanol mixture (7 : 1) with which the product was precipitated.

Bis(2-pyridylmethyl)-1-thia-4,7-diazacyclononane was prepared by the reaction between the hydrobromide salt of 1-thia-4,7-diazacyclononane and two equivalents of picolyl chloride hydrochloride in aqueous solution in the presence of excess sodium hydroxide at 0 °C, a reaction often used to add pendant arms to nitrogen atoms. The brown color of the product is due to the side reactions of traces of unreacted picolyl chloride that occur during solvent evaporation at elevated temperature (~70 °C). This substitution reaction requires that the amine group not be protonated; this defines the reaction conditions as basic. On the other hand, picolyl chloride undergoes competing reactions at pH>9, resulting in reddish or dark brown solutions. Hence, the ideal pH of the solution is slightly lower than 9. Since the reaction slowly releases HCl, sodium hydroxide must be added over a period of hours or even days to maintain the pH slightly below 9.[21,22] However, we found that maintaining the reaction at 0° is equally effective in preventing side reactions.[23] This enabled us to avoid the inconvenient slow addition of base and simply add excess base at the beginning of the reaction.

Metal complexes were prepared from the metal chlorides and the ligand in methanol. In contrast to the product of the analogous triazamacrocycle, the golden crystals of $[Fe([9]N_2Spy_2)Cl]CF_3SO_3$ are stable in air. The complex is soluble in water and polar organic solvents, such as acetonitrile, dimethyl sulfoxide, and methanol, and solutions in organic

solvents are stable showing no visible reaction upon exposure to air for days. However, the yellow aqueous solution turned red overnight in the presence of air. As expected, the manganese(II) complex is stable both in the solid state and in solutions in the presence of air.

Magnetic Moments and Electronic Spectra. The magnetic moments of iron(II) and manganese(II) complexes are 5.17 and 5.90 μ_B, respectively, indicating that both are high spin. The value for iron(II) complex is slightly higher that the spin only value (4.90 μ_B), but as expected, the magnetic moment for the manganese(II) complex is very close to the spin only value (5.92 μ_B). The conductivities for the iron(II) and manganese(II) complexes in acetonitrile are 125 and 123 $\Omega^{-1}cm^2mol^{-1}$, respectively. The values fall into the range for 1 : 1 electrolyte, 120-160 $\Omega^{-1}cm^2mol^{-1}$ in acetonitrile,[24] indicating that the chloride remains coordinated to the metal ion in the acetonitrile solutions.

The electronic spectra of the iron(II) complexes are listed in the Table 3. The iron(II) complex in acetonitrile solution, $[Fe([9]N_2Spy_2)Cl]^+$, displays an absorption maximum at 400 nm with an extinction coefficient of 1.71×10^3 M^{-1}, which can be assigned to metal-ligand charge transfer transition. When the complex is dissolved in water, a water molecule replaces the chloride forming $[Fe([9]N_2Spy_2)H_2O]^{2+}$, which exhibits a maximum absorbance at 370 nm with an extinction coefficient of 1.46×10^3 M^{-1}. The addition of two equivalents of sodium hydroxide presumably produces the hydroxo species, $[Fe([9]N_2Spy_2)OH]^+$, and is accompanied by a redshift in the absorbance of 40 nm to 410 nm (extinction coefficient, 1.66×10^3 M^{-1}). The charge transfer energy increases in the order: $H_2O>Cl^->OH^-$ (see Table 3). The changes in metal to ligand charge transfer energy are consistent with the increasing energy of the donor d-orbital that accompanies increasing ligand field strength if the latter squence is taken to be $D_{q_{OH}}>D_{q_{Cl}}>D_{q_{H_2O}}$.

Electrochemistry. Cyclic voltammagrams for the iron (II) and manganese(II) complexes in acetonitrile under nitrogen are presented in Figure 1. Within scan range from +1.5 to −1.5 V *vs.* E_{Ag/Ag^+}, the iron(II) complex exhibits a single reversible redox couple at 0.74 V *vs.* E_{Ag/Ag^+} with peak separation of 70 mV (Figure 1a), corresponding to the redox couple Fe(II)/Fe(III). Calibrating against internal ferrocene, the redox potential for the iron(II) complex, $[Fe([9]N_2Spy_2)Cl]CF_3SO_3$, is 0.66 V *vs.* NHE, which is considerably higher than that for $[Fe([9]N_3Py_2)Cl]PF_6$ (0.41 V *vs.* NHE).[1] This confirmed our prediction that the sulfur atom prefers iron(II) to iron(III) and raises the Fe(II)/Fe(III) potential to stabilize the iron(II) complex toward oxidation. The redox potential of Mn(II)/Mn(III) for the Mn(II) complex was 0.92 V *vs.* NHE, with a peak separation of 80 mV in acetonitrile solution (Figure 1b).

In aqueous solution purged with nitrogen, the iron(II) complex exhibited two redox couples at 0.13 V and 0.46 V *vs.* SCE, or 0.37 and 0.70 *vs.* NHE, (see Figure 2a), with peak separations of 90 and 50 mV, respectively. The former redox couple can be assigned to the Fe(II)/(III) aqua species, $[Fe(II)([9]N_2Spy_2)(H_2O)]^{2+}/[Fe(III)([9]N_2Spy_2)(H_2O)]^{3+}$, and the latter to the related hydroxo species, $[Fe(II)([9]N_2Spy_2)(OH)]^+/[Fe(III)([9]N_2Spy_2)(OH)]^{2+}$. In the initial scan from 0 V toward positive potentials, the absence of the anodic peak for $[Fe(II)([9]N_2Spy_2)(OH)]^+/[Fe(III)([9]N_2Spy_2)(OH)]^{2+}$ indicated that only the aqua complex, $[Fe(II)([9]N_2Spy_2)(H_2O)]^{2+}$, exists in the fully reduced solution. This is in agreement with the expectation that the iron(II) hydroxo complex, $[Fe(II)([9]N_2Spy_2)(OH)]^+$l should be a strong base. As the scanning process continues, $[Fe(II)([9]N_2Spy_2)(H_2O)]^{2+}$ is oxidized to the relatively strong acid, $[Fe(III)([9]N_2Spy_2)(H_2O)]^{3+}$, part of which undergoes deprotonation to form $[Fe(III)([9]N_2Spy_2)(OH)]^{2+}$. During the scan back to 0 V from 0.8 V *vs.* SCE $[Fe(III)([9]N_2Spy_2)(H_2O)]^{3+}$ and $[Fe(III)([9]N_2Spy_2)(OH)]^{2+}$ are reduced to $[Fe(II)([9]N_2Spy_2)(H_2O)]^{2+}$ and $[Fe(II)([9]N_2Spy_2)(OH)]^+$, respectively, so that two cathodic peaks are observed.

As discussed above, $[Fe(II)([9]N_2Spy_2)(OH)]^+$ cannot exist in the bulk of the solution at the experimental pH but must capture a proton to form $[Fe(II)([9]N_2Spy_2)(H_2O)]^{2+}$. However, when scanning continues, a new anodic peak appears at 0.17 V vs. SCE, presumably resulting from the oxidation of $[Fe(II)([9]N_2Spy_2)(OH)]^+$ to $[Fe(III)([9]N_2Spy_2)(OH)]^{2+}$ in the vicinity of the electrode. From the integration of peak areas it was estimated that almost half of the $[Fe(II)([9]N_2Spy_2)(OH)]^+$ was oxidized prior to neutralization by protons. It is interesting that the protonation of $[Fe(II)([9]N_2Spy_2)(OH)]^+$ at the electrode is so slow; i.e., having a half life of several seconds. In the third scan, the voltammagrams were unchanged from the second scan. On extending the scan range so that the lower limit was −0.75 V *vs.* SCE, the longer scan time allowed the complete protonation of $[Fe(II)([9]N_2Spy_2)(OH)]^+$ species, and the second anodic peak disappeared (see Figure 2b). In this case, the voltammogram for the second scan is virtually identical

Table 3. Electronic spectra and redox potentials of $[Fe(II)([9]N_2Spy_2)X]^{n+}$

Complexes	$[Fe(II)([9]N_2Spy_2)X]^{n+}$		
X	H_2O	Cl	OH
λ_{max} (nm)	370	400	410
ν (cm^{-1})	27,027	25,000	24,390
ε ($\times10^3$ M^{-1})	1.46	1.71	1.66
$E_{1/2}$ (V *vs.* NHE)	0.70	0.66	0.37

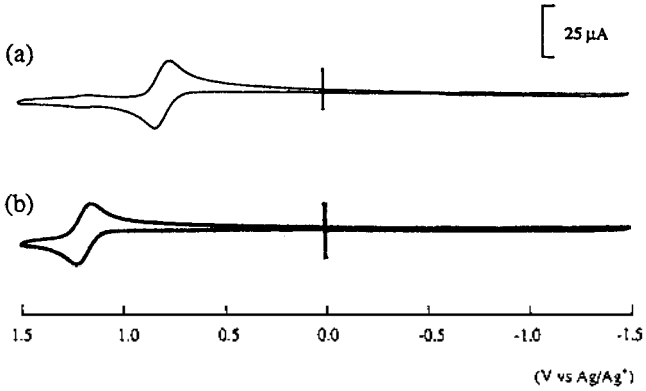

Figure 1. Cyclic voltammograms of (a) $[Fe([9]N_2Spy_2)Cl]CF_3SO_3$ and (b) $[Mn([9]N_2Spy_2)Cl]CF_3SO_3$ in acetonitrile (2 mM) purged with nitrogen. Scan rate, 100 mV/s; working electrode, glassy carbon; secondary electrode, platinum wire; reference electrode, silver wire; supporting electrolyte, 0.1 M t-Bu_4NBF_4.

with the first one, differing only by the presence of a small bump at far right in the first scan, which probably resulted from an impurity such as oxygen on the surface of the polished electrode.

Sodium hydroxide was added to the aqueous solution in order to establish the hydroxo complexes as the species involved in the redox couple at 0.13 V *vs.* SCE. The peaks at more positive potential became smaller as a sodium hydroxide solution was added to the solution, and finally disappeared when one equivalent of NaOH was added (Figure 2c). At the same time, the peaks around 0.13 V *vs.* SCE became larger as sodium hydroxide was added. From these results it is concluded that the peaks at more positive potentials result from the redox reaction of the aqua species while the hydroxo species are responsible for the redox peaks around 0.13 V *vs.* SCE. This electro-chemical system is summarized in Scheme 2.

As seen above, the nature of the monodentate ligand affects the redox potential of the iron complex. The potentals for $[Fe(II)([9]N_2Spy_2)(X)]^{n+}$ (X=Cl^-, OH^-, and H_2O) increase in the following order: H_2O>Cl >OH . This

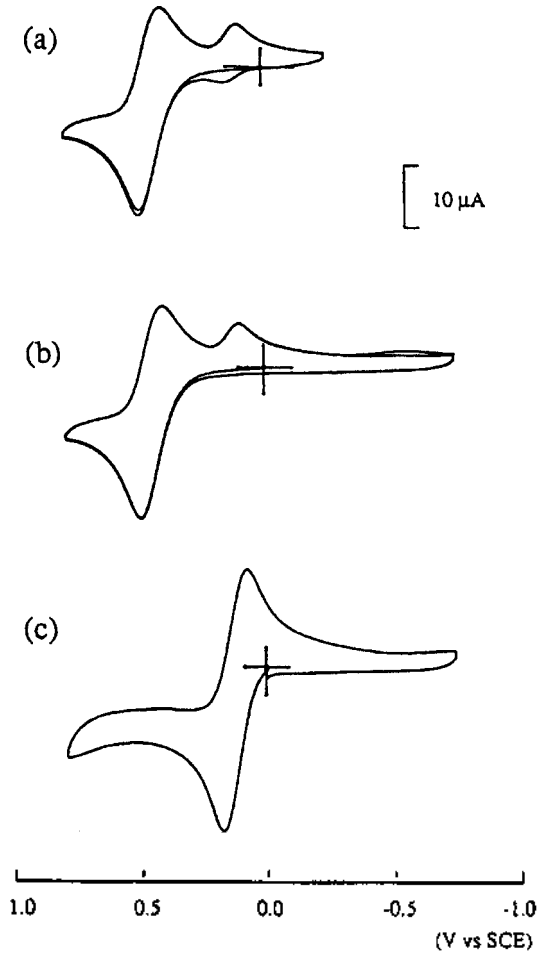

Figure 2. Cyclic voltammograms of $Fe([9]N_3py_2)(PF_6)$ in aqueous solution under nitrogen: a) scan range, −0.25 to +0.8 V *vs.* SCE; b) scan range, −0.75 to +0.8 V *vs.* SCE; c) 1 equivalent of NaOH was added. Scan rate, 100 mV/s; working electrode, glassy carbon; secondary electrode, platinum wire; reference electrode, saturated calomel electrode; supporting electrolyte, 0.1 M $NaClO_4$.

order is the same as that observed for the charge transfer energy of the electronic spectrum, discussed in the last section (see Table 3). The correlation between the spectral charge transfer energy and the redox potential has been observed for other complexes.[1,25] For a given metal, charge transfer transitions decrease in energy as the metal becomes more easily oxidizable.[25] Although there is no defined relationship between the charge transfer and redox potential, their correlation is not too difficult to understand. The easier it is for and electron to transfer to a certain π^* orbital, the easier it is to lose the electron and the potential required to remove the electron is lowered.

At scan rates < 200 mV/s in 2 M KCl aqueous solution, $[Fe(II)[9]N_2Opy_2Cl](PF_6)$ (see Structure) exhibited a redox couple at 0.81 vs. SCE;[26] this value is higher than the potential found for $[Fe(II)[9]N_2Spy_2Cl](CF_3SO_3)$ in acetonitrile or aqueous solutions. The only difference in the ligand is that an O atom is replaced by an S atom on the cyclononane ring. This result indicates that the oxygen donor stabilizes Fe(II) oxidation state toward oxidation more than the sulfur does.

Crystal structure of $[Fe([9]N_2Spy_2)Cl]CF_3SO_3$ (9) and $[Mn([9]N_2Spy_2)Cl]CF_3SO_3$ (10). Before considering the structures themselves, it is useful to examine the conformations of the pendant arms on a diazacyclononane ring. Figure 3a shows the superposition of two conformations of these pendant arms as viewed from above. Two effects are important here. Because of the staggered conformation of the ring C-C bonds, C2 is closer than C1 to the plane defined by N1-N2-N3, as seen in the side view in Figure 3b. As a result, the N1-C3 bond is inclined relative to the N1-M direction (*i.e.* the N1-C3-M plane is not perpendicular to the N1-N2-N3 plane, even if M is centrally located above the N1-N2-N3 ring).

The pendant pyridyl attached to C3 takes up one of the three positions giving a staggered conformation for the N1-C3 bond (the two H-atoms occupying the other positions). In one of these positions, the arm is directed away from the metal and cannot coordinate. In the two coordinating conformations, the arm is directed either to the opposite side of the N1-C3 line as the metal or the same side (as seen in Figures 3a and b). These conformations are here named, respectively, α (solid line) and β (dashed line).

Although the conformations differ only in the orientation of the pendant arm at C3, they have a major effect on the

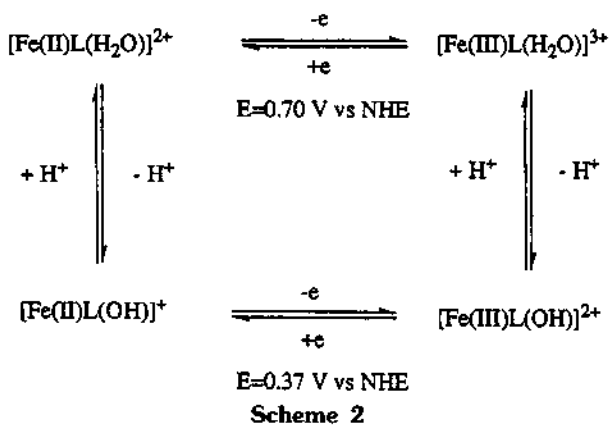

Scheme 2

metal coordination geometry. In the β-conformation, the pendant N-M bond is positioned almost over the corresponding ring N-M bond, leading to a trigonal prismatic geometry with a twist angle close to 0° (The twist angle is defined as the angle between the upper and lower M-N bonds projected on the plane defined by N1-N2-N3). By contrast, in the α-conformation, the twist angle is close to 60° and the geometry is distorted octahedral. These geometrical differences are clearly seen form the top view (Figure 3a). These different conformations also produce significant differences in the '*trans*' N-M-N angles, 180° for octahedral and approximately 130° for trigonal prismatic geometry (the value obtained by twisting one face of an octahedron).

This conformational distinction is relevant not only to the pendant arms on triazacyclononane but also to many other systems in which two inequivalent methylene groups are connected to an N atom carrying a pendant arm. It is also applicable to a variety of pendant arms, though if the arm contains more than two C atoms between the ligating atoms, its greater flexibility may reduce the effect on the metal geometry. In particular, of course, it is applicable to the 1-thia-4,7-diazacyclononane compound presented here.

Views of the crystal structures are given in Figure 4. In both structures, the coordination geometries are closer to trigonal prismatic than octahedral geometry with their 2-pyridylmethyl groups in the β conformation. In contrast, the two 2-pyridylmethyl groups in the Ni(II) complex[3] adopt the α-conformation (Figure 5), and the coordination geometry is only slightly distorted from octahedral.

The twist angles are listed in Table 4 (defined as in Figure 6) are useful in comparing the coordination geometries of the complexes. Since the Cl and S atoms are not linked together, the Cl atom can adopt a position to minimize steric hindrance. Although both the iron and manganese complexes adopt the β-conformation, the S-M-Cl twist angles (ϕ^1) are nearer to 60° than to the value of 0° that is expected for a trigonal prism. This is presumably the result of repulsion between the relatively large S and Cl atoms. The twist angle ϕ^2 (27.3° for Mn and 30.1° for Fe)

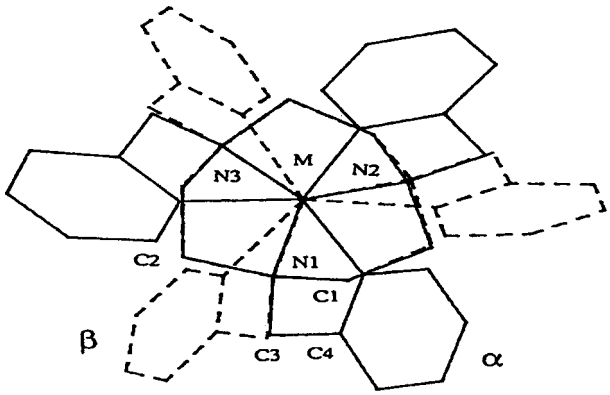

Figure 3. (a) Top view of a tri-azacyclononane with three attached 2-pyridylmethyl pendant arms in two alternative conformations: α-conformation (solid line) with metal and pendant arm on the same side of the N1-C3 line and β-conformation (dashed line) with metal and pendant arm on the opposite side of the N1-C3 line. (b) Side-on view showing only one 2-methylpyridyl group for clarity (α-conformation in solid line and β-conformation in dotted line).

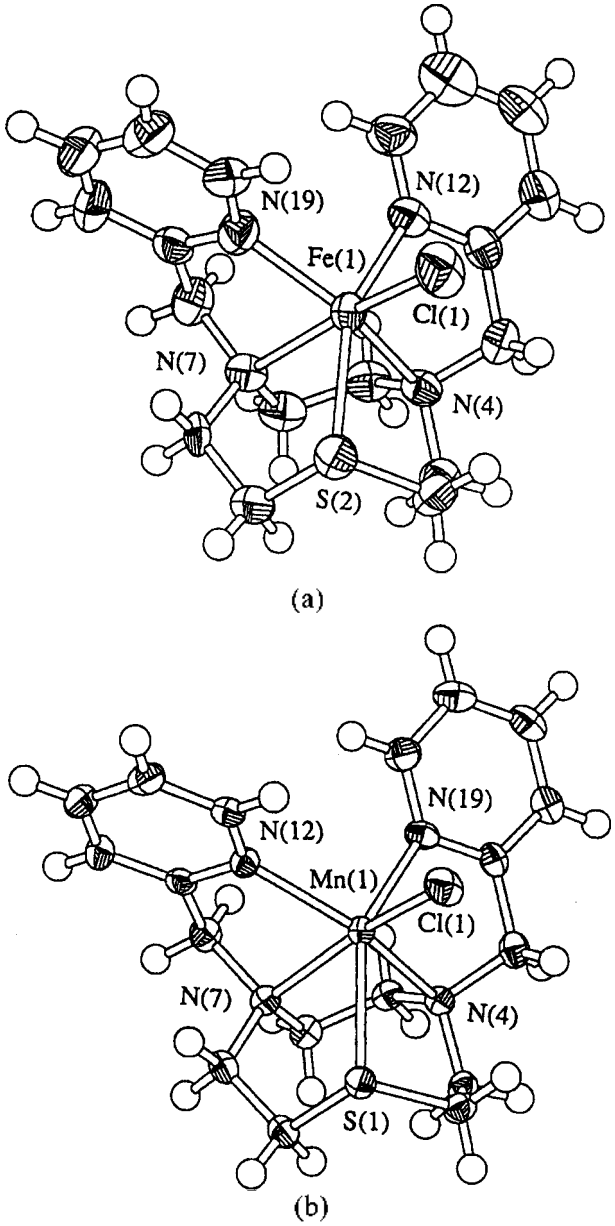

Figure 4. Views of the structures of (a) [Fe([9]N_3Spy_2)Cl](CF_3SO_3) and (b) [Mn([9]N_3Spy_2)Cl](CF_3SO_3).

is always greater than ϕ^3 (19.6° for Mn and 23.1° for Fe), probably due to the repulsion between the chloride ion and the pyridyl group. In the nickel(II) analogue, the N(sp^3)-Ni-N(sp^2) twist angles are almost the same as in $(Ni[9]N_3py_3)^{2+}$, and the S-Ni-O twist angle is very close to 60°.

These results clearly show that the metal ion size influences the conformations of the pendant arm chelate rings, as previously observed for complexes of 1,4,7-tris(2-pyridylmethyl)-1,4,7-triazacyclononane.[21,22] With nickel(II) and low spin iron(II), the pendant arms adopt α-conformations while high spin manganese(II) coordinates in the β-conformation. This effect of metal ion size has also been studied by molecular mechanics.[5] The calculations showed that a metal ion with M-N(sp^3) distance of 2.08 is ideal for the α-conformation for 2-pyridylmethyl group, while the best fit M-N(sp^3) distance for the β-conformation is 2.16. Thus the present results add to the evidence from previous crystal structures that larger metal ions favor the β-conformation.

The three five-membered chelate rings in the 1-thia-4,7-diazacyclononane unit itself adopt the δδδ or λλλ conformations in both $[Fe(II)([9]N_2Spy_2)Cl]^{2+}$ and $[Mn(II)([9]N_2Spy_2)Cl]^{2+}$, as also observed for the nickel(II) analogue[3] and in $[Fe(II)N_2Opy_2Cl]^{2+}$.[26] However, δδλ or δλλ

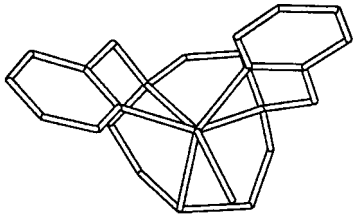

(a) Pendant Arms with β-Conformation in $[Fe([9]N_2Spy_2)Cl]^+$

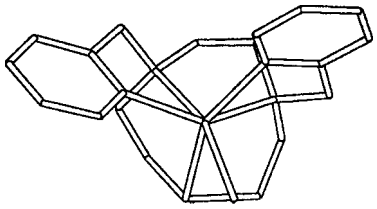

(b) Pendant Arms with β-Conformation in $[Mn([9]N_2Spy_2)Cl]^+$

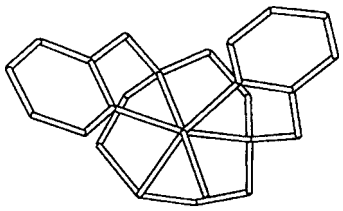

(c) Pendant Arms with α-Conformation in $[Ni([9]N_2Spy_2)(H_2O)]^{2+}$

Figure 5. Conformations of the pendant arms in iron(II), manganese(II), and nickel(II) complexes with $[9]N_2Spy_2$.

Table 4. Twist angles (degree)[a]

	X-M-Y	N(sp^3)-M-N(sp^2)		
	ϕ^{1b}	ϕ^2	ϕ^3	Ref.
$[Fe([9]N_2Spy_2)Cl]CF_3SO_3$ (6)	44.2	30.1	23.1	this work
$[Mn([9]N_2Spy_2)Cl]CF_3SO_3$ (7)	41.4	27.3	19.6	this work
$[Ni([9]N_2Spy_2)OH_2]PF_6$	57.4	47.1	46.6	6, 7
$[Fe([9]N_2Opy_2)Cl]PF_6$	39.6	34.0	20.2	26
$[Mn([9]N_3py_3)]ClO_4$		19.6		21, 22
$[Fe([9]N_3py_3)]ClO_4$		49.0		21, 22
$[Ni([9]N_3py_3)]ClO_4$		46.8		21, 22
Regular octahedron		60		
Trigonal prism		0		

[a] Twist angles are determined from the M-N angles projected on the plane defined by the ligating atoms on the cyclonanane rings. [b] ϕ^1, ϕ^2 and ϕ^3 are defined respectively as the twist angle between (1) the ring hetero-atom (O or S) and the unidentate ligand (Cl or H_2O), (2) between N(sp^3) and N(sp^2) in the chelate ring closer to the unidentate ligand (3) between N(sp^3) and N(sp^2) in the other chelate ring (see Figure 6).

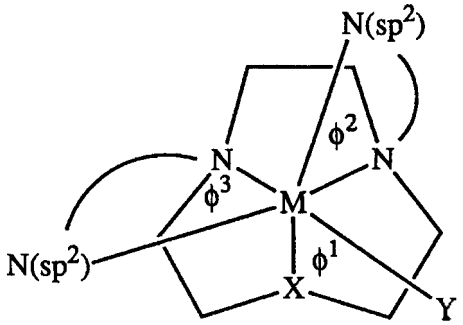

X = S, NH, O
Y = Cl, H_2O

Figure 6. Identification of the three twist angles in the metal complexes $[M([9]N_2Xpy_2)Y]$.

Table. 5. Selected bond lengths (Å) and bond angles (degree)

Fe(1)-Cl(1)	2.332(3)	Fe(1)-S(1)	2.521(3)
Fe(1)-N(4)	2.227(6)	Fe(1)-N(7)	2.299(7)
Fe(1)-N(12)	2.185(6)	Fe(1)-N(19)	2.137(6)
Mn(1)-Cl(1)	2.400(1)	Mn(1)-S(1)	2.621(1)
Mn(1)-N(4)	2.303(3)	Mn(1)-N(7)	2.382(3)
Mn(1)-N(12)	2.195(3)	Mn(1)-N(19)	2.248(3)
Cl(1)-Fe(1)-S(1)	86.9(1)	Cl(1)-Fe(1)-N(4)	110.4(2)
S(1)-Fe(1)-N(4)	82.8(2)	Cl(1)-Fe(1)-N(7)	163.7(2)
S(1)-Fe(1)-N(7)	79.3(2)	N(4)-Fe(1)-N(7)	76.7(2)
Cl(1)-Fe(1)-N(12)	89.6(2)	S(1)-Fe(1)-N(12)	155.1(2)
N(4)-Fe(1)-N(12)	75.4(2)	N(7)-Fe(1)-N(12)	106.6(2)
Cl(1)-Fe(1)-N(19)	100.4(2)	S(1)-Fe(1)-N(19)	110.1(2)
N(4)-Fe(1)-N(19)	147.4(2)	N(7)-Fe(1)-N(19)	76.6(2)
N(12)-Fe(1)-N(19)	94.8(2)		
N(12)-Mn(1)-N(19)	97.3(1)	N(12)-Mn(1)-N(4)	145.1(1)
N(19)-Mn(1)-N(4)	73.7(1)	N(12)-Mn(1)-N(7)	75.9(1)
N(19)-Mn(1)-N(7)	108.6(1)	N(4)-Mn(1)-N(7)	75.5(1)
N(12)-Mn(1)-Cl(1)	100.9(1)	N(19)-Mn(1)-Cl(1)	89.9(1)
N(4)-Mn(1)-Cl(1)	112.4(1)	N(7)-Mn(1)-Cl(1)	161.4(1)
N(12)-Mn(1)-S(1)	111.9(1)	N(19)-Mn(1)-S(1)	150.8(1)
N(4)-Mn(1)-S(1)	80.9(1)	N(7)-Mn(1)-S(1)	77.8(1)
Cl(1)-Mn(1)-S(1)	86.65(3)		

Table 6. M-N(sp^3) and M-N(sp^2) distances (X=unidentate ligand, Cl or OH_2; Y=ring hetero-atom, S or O)

Complexes	M-N(sp^3) (Å) *trans* to X		Difference (Å) *cis* to X
[Fe([9]N_2Spy_2)Cl]CF_3SO_3 (**9**)	2.299(7)	2.227(6)	0.072
[Mn([9]N_2Spy_2)Cl]CF_3SO_3 (**10**)	2.382(3)	2.303(3)	0.079
[Ni([9]N_2Spy_2)(H_2O)]PF_6	2.088(13)	2.069(13)	0.019
[Fe([9]N_2Opy_2)Cl]PF_6	2.266(7)	2.206(6)	0.060
Complexes	M-N(sp^3) (Å) *trans* to Y		Difference (Å) *cis* to Y
[Fe([9]N_2Spy_2)Cl]CF_3SO_3 (**9**)	2.185(6)	2.137(6)	0.048
[Mn([9]N_2Spy_2)Cl]CF_3SO_3 (**10**)	2.248(3)	2.195(3)	0.053
[Ni([9]N_2Spy_2)(H_2O)]PF_6	2.098(12)	2.030(13)	0.068
[Fe([9]N_2Opy_2)Cl]PF_6	2.179(6)	2.149(6)	0.030

conformations have been found in the structures of the Pd (II), and Pt(II) analogues and other complexes such as [LMo$(CO)_2$NO]PF_6[27] and Cu$(L)_2NO_3$,[28] where L=1-thia-4,7-diazacyclononane.

Selected bond lengths and bond angles of the complexes are given in Table 5. Both the M-S and M-Cl distances are shorter for iron(II) than manganese(II), though the difference is significantly larger for the bond to S (0.100 compared to 0.068 Å). In both complexes, the M-N(sp^3) bond lengths vary, with the bonds to the nitrogen *trans* to the chloride ligand longer by 0.07-0.08 Å. This so called *trans* influence[29] has also been observed in [Fe([9]aneN_2O)Cl](PF_6). In contrast, in [Ni([9]N_2Spy_2)(H_2O)]$(ClO_4)_2$ the difference between the two Ni-N(sp^3) bonds is marginal (2.088(13) and 2.069(13) Å) (summarized in Table 6). Thus the Cl^- has a greater *trans* influence than does a water molecule. A similar influence is seen in the M-N(sp^2) distances, with the bond *trans* to S being somewhat lengthened, while O has a smaller *trans* influence. From Table 6, it can be seen that the sequences of the *trans* influence on M-N(sp^3) and M-N(sp^2) in these complexes are $Cl^- > H_2O >$ py and $SR_2 > OR_2 > NR_3$, respectively.

Acknowledgment. The support of this research by the Monsanto Company is greatly appreciated. We thank Professor M. Hursthouse, University of Cardiff, for providing data from the SERC Crystallographic Service.

Supplementary material available. H-atom coordinates, thermal parameters and the remaining bond lengths and angles are available from the Cambridge Crystallographic Data Center.

References

1. Fee, J. L.; McClune, F. J. *Mechanics of Oxidizing Enzymes*; Singer, T. P.; Ondarza, R. N., Eds.; Elsevier/North Hooland: Amsterdam, 1878; p 273.
2. Fee, J. L.; McClune, F. J.; O'Neill, P.; Fiekden, E. M. *Biochem. Biophys. Res. Commun.* **1981**, *100*, 277.
3. Bull, C.; Fee, J. A. *J. Am. Chem. Soc.* **1985**, *107*, 3295.
4. Lah, M. S.; Dixon, M. M.; Pattridge, K. A.; Stallings, W. C.; Grr, J. A.; Ludwig, M. L. *Biochem.* **1995**, *34*, 1646.
5. Zhang, D. Ph.D. Dissertation, University of Kansas, 1994.
6. Wasielewski, K.; Mattes, R. *Acta Crystallogr. Sect. C: Cryst. Struct. Commun.* **1990**, *C46*(10), 1826.
7. Wasielewski, K.; Mattes, R. *Z. Anorg. Allg. Chem.* **1993**, *619*, 158.
8. Hope, D. B.; Horncastle, K. C. *J. Chem. Soc. (C)* **1966**, 1098.
9. Dietrich, B.; Hosseini, M. W.; Lehn, J.-M.; Sesions, R. B. *Helv. Chim. Acta* **1985**, *68*, 289.
10. Evans, D. F. *J. Chem. Soc.* **1959**, 2003.
11. Sur, S. K. *J. Magn. Reson.* **1989**, *82*, 169.
12. Drago, R. S. *Physical Methods*, 2nd Ed.; Saunder College Publishing: Orlando, 1992; p 472.
13. Cosier, J.; Glazer, A. M. *J. Appl. Cryst.* **1986**, *19*, 105.
14. Alcock, N. W.; Marks, P. J. *J. Appl. Cryst.* **1993**, *27*, 200.
15. Sheldrick, G. M. *SHELXTL PLUS user's manual*; Nicolet Instr. Co.: Madison, Wisconsin, 1986.
16. Sheldrick, G. M. *J. Appl. Cryst.* **1996**, in press.
17. Hoffman, P.; Mattes, R. *Inorg. Chem.* **1989**, *28*, 2092.
18. Hart, S. M.; Boeyens, J. C. A.; Michael, J. P.; Hancock, R. D. *J. Chem. Soc., Dalton Trans.* **1983**, 1601.
19. Mills, E.; Bogert, M. T. *J. Chem. Soc.* **1940**, 1173.
20. Schroder, M. Personal communication.
21. Christiansen, L.; Hendrickson, D. N.; Toftlund, H.; Wilson, S. R.; Xie, C. L. *Inorg. Chem.* **1986**, *25*, 2813.
22. Wieghardt, K.; Schoffmann, E.; Nuber, N.; Weiss, J. *Inor. Chem. 1986, 25*, 4877.
23. Zhang, D.; Busch, D. H. *Inorg. Chem.* **1994**, *33*, 5138.
24. Geary, W. J. *Coord. Chem. Rev.* **1991**, 81.
25. Lever, A. B. P. *Inorganic Electronic Spectroscopy*; Elsevier: Amsterdam, 1984; p 206.
26. Szulbinski, W. S.; Warburton, P. R.; Busch, D. H. *Inorg. Chem.* **1993**, *32*, 297.
27. Hoffmann, P.; Mattes, R. *Inorg. Chem.* **1989**, *28*, 2092.
28. Boeyens, J. C. A.; Dobson, S. M.; Hancock, R. D. *Inorg. Chem.* **1985**, *24*, 3073.
29. Cotton, F. A.; Wilkinson, G. *Advanced Inorganic Chemistry*, 5th Ed.; Johen Wiley & Sons: New York, p 300.